Peptide-Induced Formation of Cholesterol-Rich Domains†

Richard M. Epand,*,‡ Brian G. Sayer,§ and Raquel F. Epand‡

Department of Biochemistry, McMaster University, Hamilton, Ontario L8N 3Z5, Canada, and Department of Chemistry, McMaster University, Hamilton, Ontario L8S 4M1, Canada

Received September 3, 2003; Revised Manuscript Received October 9, 2003

ABSTRACT: The peptide *N*-acetyl-LWYIK-amide causes the reorganization of bilayers of phosphatidylcholine and cholesterol to produce domains enriched in cholesterol. At a cholesterol mol fraction of 0.5, addition of *N*-acetyl-LWYIK-amide results in the formation of cholesterol crystallites. Addition of this peptide to mixtures of 1-stearoyl-2-oleoylphosphatidylcholine with lower mol fractions of cholesterol results in an increase in the enthalpy of the chain melting transition of the phospholipid, indicating the depletion of cholesterol from a domain in the membrane. The peptide binds to membranes both with and without cholesterol. However, ^{1}H magic-angle spinning (MAS) nuclear Overhauser effect spectroscopy (NOESY) indicates that in the presence of cholesterol the peptide has greater penetration into the bilayer. ^{13}C MAS NMR indicates that the peptide has stronger interactions with the A ring of cholesterol than it does with the interior of the bilayer. These results are in contrast with those of another peptide, *N*-acetyl-KYWFYR-amide, which does not promote the formation of cholesterol crystallites and does not show preferential interaction with cholesterol by NMR. Therefore, cholesterol can promote the insertion of *N*-acetyl-LWYIK-amide into a membrane and this peptide will sequester cholesterol into domains. These properties help to explain the observation that this sequence is found to be important in causing the fusion protein of human immunodeficiency virus (HIV) to sequester into raft domains in biological membranes.

There is considerable current interest in the formation and properties of cholesterol-rich domains in biological membranes (for a recent series of reviews, see ref *1*). One type of cholesterol-rich domain is the caveolae that are enriched in the lipids cholesterol and sphingomyelin. Domains of similar lipid composition, termed rafts, are thought to also be floating in the plasma membrane. These domains sequester certain proteins but not others. Most GPI-anchored proteins and many palmitoylated proteins are found in cholesterol-rich domains (*2*). There is also evidence to suggest that both the mechanical properties and the avoidance of length mismatch between transmembrane segments and bilayer thickness contribute to the partitioning of proteins into different membrane domains (*3*). In addition, it has been suggested that some amino acid sequences also favor partitioning into raft domains. There is a structural motif present in the V3 loop of HIV-1[1] gp 120, the human prion protein (PrP), and the Alzheimer β-amyloid peptide (*4*) as well as other proteins (*5*) that is believed to target these proteins to raft domains by having affinity for sphingomyelin. However, cholesterol is also required for the high-affinity binding of one of these segments to membranes, the V3 loop of gp120 (*6*). There may also be other cholesterol-rich domains in membranes that do not fit the definition of rafts because they do not have a high concentration of sphingomyelin, they are not in the liquid-ordered phase, and they are not insoluble in 1% Triton X-100 at 4 °C. Certain proteins and peptides have affinity for cholesterol-rich domains. It has been shown that a protein found in neuronal rafts, NAP-22, binds to membranes containing cholesterol (*7*, *8*). It has also been found that a toxic peptide, perfringolysin O, binds to cholesterol-rich domains in membranes (*9*−*11*). For another group of proteins, there is evidence for the existence of a consensus sequence, having the pattern -L/V-(X)(1−5)-Y-(X)(1−5)-R/K-, in which (X)(1−5) represents 1−5 residues of any amino acid that recognizes cholesterol (*12*). The HIV-1 fusion protein gp41 has a segment consistent with this consensus sequence that is adjacent to the transmembrane anchor. This segment contains the sequence LWYIK and has been shown to promote membrane fusion by mutational studies of the intact viral protein (*13*) as well as with the use of a 20-amino acid synthetic peptide (*14*). This synthetic peptide contains the LWYIK sequence at the carboxyl terminal end, but the amino terminal segment of this peptide is also required for membrane fusion, perhaps by facilitating oligomerization of gp41 (*50*). Cholesterol was found to be required for HIV infection (*15*−*17*) as well as for fusion promoted by the synthetic peptide (*14*). Depletion of cholesterol from HIV results in loss of their infectivity (*51*).

† This work was supported by a grant from the Canadian Institutes of Health Research, Grant MT-7654.

* To whom correspondence should be addressed: e-mail epand@mcmaster.ca.

‡ Department of Biochemistry, McMaster University.

§ Department of Chemistry, McMaster University.

[1] Abbreviations: PC, phosphatidylcholine; DO, dioleoyl; PO, 1-palmitoyl-2-oleoyl; SO, 1-stearoyl-2-oleoyl; DNS-PE, *N*-[5-(dimethylamino)-naphthalene-1-sulfonyl]-1,2-dihexadecanoyl-*sn*-glycero-3-phosphoethanolamine, triethylammonium salt; CP, cross polarization; MAS, magic angle spinning; MLV, multilamellar vesicle; LUV, large unilamellar vesicle; SUV, small unilamellar vesicle; DSC, differential scanning calorimetry; T_m, transition temperature; ΔH_{cal}, calorimetric enthalpy; HIV-1, human immunodeficiency virus type 1; EDTA, ethylenediaminetetraacetic acid; Hepes, *N*-(2-hydroxyethyl)piperazine-*N*′-2-ethanesulfonic acid; NOESY, nuclear Overhauser effect spectroscopy; PIPES, piperazine-*N*,*N*′-bis(2-ethanesulfonic acid); 1-D and 2-D, one- and two-dimensional.

10.1021/bi035587j CCC: $25.00
Published on Web 11/14/2003

The role of the short sequence LWYIK for binding to cholesterol has been demonstrated by measuring the binding of maltose binding protein fusion proteins to cholesterol−hemisuccinate agarose (*18*). In contrast to LWYIK, the sequence KYWFYR, found in caveolin-1, a major component of caveolae, is important in sequestering the protein to membranes but is not sufficient to target the protein to the cholesterol-rich domain of caveolae (*19*). In the present work we characterize the interaction of the isolated peptides *N*-acetyl-LWYIK-amide and *N*-acetyl-KYWFYR-amide with cholesterol in model membranes.

EXPERIMENTAL PROCEDURES

Materials. The peptide *N*-acetyl-LWYIK-amide was synthesized by Biosource (Hopkinton, MA) and by SynPep Corporation (Dublin, CA) and purified to >98% purity by high-performance liquid chromatography (HPLC). The peptide *N*-acetyl-KYWFYR-amide was synthesized by Dalton Chemical Laboratories, Toronto, Canada, to >95% purity. Phospholipids were purchased from Avanti Polar Lipids (Alabaster, AL), except for the *N*-[5-(dimethylamino)-naphthalene-1-sulfonyl]-1,2-dihexadecanoyl-s*n*-glycero-3-phosphoethanolamine, triethylammonium salt (DNS-PE), which was purchased from Molecular Probes (Eugene, OR). Cholesterol was purchased from Avanti or from NuChek Prep (Elysian, MN).

Preparation of Samples for DSC and NMR Experiments. Phospholipid and cholesterol were codissolved in chloroform/methanol (2/1 v/v). For samples containing peptide, an aliquot of a solution of the peptide in methanol was added to the lipid solution in chloroform/methanol. The solvent was then evaporated under a stream of nitrogen with constant rotation of a test tube so as to deposit a uniform film of lipid over the bottom third of the tube. Last traces of solvent were removed by placing the tube under high vacuum for at least 2 h. The lipid film was then hydrated with 20 mM PIPES, 1 mM EDTA, and 150 mM NaCl with 0.002% NaN_3, pH 7.40, and suspended by intermittent vortexing and heating to 50 °C over a period of 2 min under argon. Samples used for NMR analysis were hydrated with the same buffer made in ^2H_2O and adjusted to a pH meter reading of 7.0 (pD = 7.4) and incubated at least 24 h at 4 °C to allow conversion of anhydrous cholesterol crystals to the monohydrate form. For the NMR measurements, the samples were spun in an Eppendorf centrifuge at room temperature. The resulting hydrated pellet was transferred to a 18 × 4 mm ZrO_2 rotor, attempting to pack the maximal amount of lipid into the rotor while maintaining it wet.

Differential Scanning Calorimetry. Measurements were made on a nano differential scanning calorimeter (Calorimetry Sciences Corp., American Fork, UT). The scan rate was 2 °C/min and there was a delay of 5 min between sequential scans in a series to allow for thermal equilibration. The features of the design of this instrument have been described (*20*). DSC curves were analyzed by use of the fitting program DA-2, provided by Microcal Inc. (Northampton, MA), and plotted with Origin, version 5.0.

Large Unilamellar Vesicles. Lipid films were made as described above for DSC and NMR samples. Films were hydrated with buffer, vortexed extensively at room temperature, and then subjected to five cycles of freezing and thawing. The homogeneous lipid suspensions were then further processed by 10 passes through two stacked 0.1 μm polycarbonate filters (Nucleopore Filtration Products, Pleasanton, CA) in a barrel extruder (Lipex Biomembranes, Vancouver, BC) at room temperature. LUVs were kept on ice and used within a few hours of preparation. Lipid phosphorus was determined by the method of Ames (*21*).

Dissociation of N-Acetyl-LWYIK-amide from Membranes. The resonance energy transfer assay between the Trp residue of *N*-acetyl-LWYIK-amide and the dansyl group on DNS-PE was used to assess the dissociation of the peptide from a membrane. LUVs were prepared containing an equimolar mixture of POPC and cholesterol with 5 mol % DNS-PE added. The LUVs were diluted to a concentration of 300 μM lipid (30 μM peptide) and the fluorescence emission was measured with an excitation wavelength of 290 nm. The change of emission intensity at 520 nm was recorded as a function of time at 25 °C.

Centrifugation Assay for Membrane Binding of N-Acetyl-LWYIK-amide. The fraction of peptide bound to the lipid after three heating and cooling cycles between 0 and 50 °C was determined by separating the free peptide by centrifugation. The vesicles with bound peptide were pelleted at 200000*g* for 90 min at 25 °C. A clear supernatant was separated from the solid pellet and assayed for peptide by absorption at 278 nm. The absorption of a blank was subtracted and a baseline, set at 350 nm for each sample, was used to correct for residual scattering.

Tryptophan Fluorescence Studies. The peptide was dissolved in 10 mM Hepes buffer, 0.14 M NaCl, and 0.1 mM EDTA, pH 7.4. Dilutions were made from a 1 mg/mL stock solution. The concentration of peptide was determined by absorbance at 280 nm by use of an extinction coefficient calculated from the amino acid content (*22*). Excitation wavelengths of 280 and 295 nm were used, with 4 nm bandwidth in excitation and 8 nm in emission. Polarizers set to 90° in excitation and 0° in emission were used to reduce stray light. Fluorescence emission spectra were measured by use of ultrasensitive quartz mirror microcuvettes (N. L. Vekshin, Institute of Cell Biophysics, Pushchino, Russia). Spectra were determined at 25 °C on an SLM Aminco Bowman AB-2 spectrofluorometer. The spectra were corrected for instrumental factors and a buffer blank was subtracted. Inner filter effect corrections were applied. When the peptide was incorporated into the lipid film, they were then hydrated in Hepes buffer, vortexed and sonicated to make SUVs. The same concentration of SUVs of lipid without peptide was used as a blank. Concentration of the peptide in the cuvette for all samples was 150 μM.

^{1}H NOESY MAS NMR. High-resolution MAS spectra were acquired by use of a 4 mm zirconia rotor spinning at 4 kHz in a Bruker DRX 500 NMR spectrometer. Probe temperature was 24 ± 1 °C. The 2D-NOESY spectra were obtained with mixing times of 50 and 300 ms. Resonances were assigned on the basis of reports of phosphatidylcholine (*23*), cholesterol (*24*), and amino acid residues (*25*). The structures of the lipids used are given in Figure 1, numbered for identification purposes.

^{13}C CP/MAS NMR. A 4 mm zirconia rotor was placed in a Bruker Avance 300 spectrometer operating at 75.48 MHz for ^{13}C and equipped with CP-MAS capabilities. The spectra were referenced to an external standard of glycine crystals,

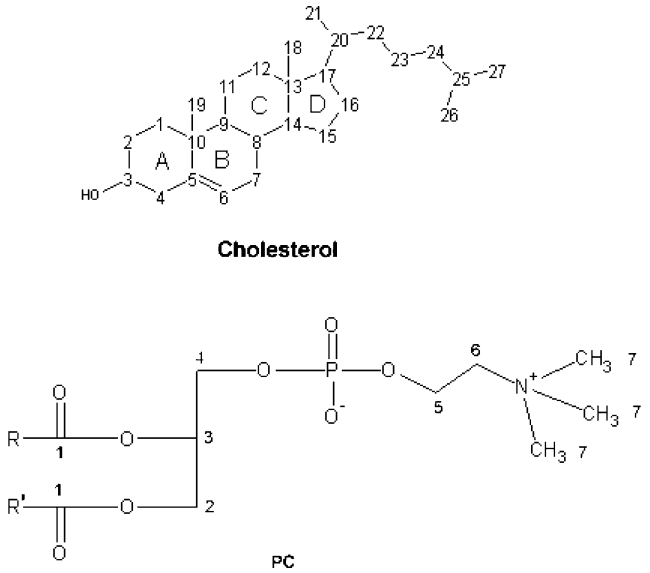

FIGURE 1: Chemical structures of cholesterol and phosphatidylcholine (PC). The numbering system for cholesterol follows IUPAC rules, while the numbering of PC is arbitrary and is used only for identification purposes in the tables and figures. R and R′ are the acyl chains.

assigning a chemical shift of 176.14 ppm for the carbonyl carbon. Samples were spun at 5 kHz. The temperature inside the rotor was 25 ± 1 °C. The power levels used for cross-polarization corresponded to a 4 μs $\pi/2$ pulse. The Hartmann−Hahn match was established on the sample of glycine. Continuous-wave decoupling at an increased power level was used during acquisition. Some experiments were repeated to verify the stability and reproducibility of the cross-polarization. Generally each spectrum was obtained with 12 000 scans and processed with 1 Hz line broadening.

Direct Polarization. Single-pulse excitation with high-power proton decoupling was used with a 4 μs pulse for ^{13}C and the proton frequency was optimized for decoupling. A recycle time of 5 s was used.

RESULTS

DSC Evidence for Peptide-Induced Segregation of Cholesterol. Cholesterol forms crystals when the mole fraction of sterol in a membrane exceeds a certain value. The solubility limit of cholesterol is very dependent on the nature of the phospholipid with which it is mixed. Cholesterol crystals are generally not observed in mixtures with phosphatidylcholine (PC) at cholesterol mole fractions of 0.5 or below (*26*, *27*), the only exception to this being PC containing polyunsaturated acyl chains (*28*−*30*). Cholesterol can form anhydrous crystals that exhibit a polymorphic crystalline transition at 38 °C on heating as well as cholesterol monohydrate crystals that undergo a dehydration generally at about 80 °C when in pure form (*31*) or when mixed with phospholipids at high mole fractions, although in the presence of certain membrane components the transition temperature for the dehydration of cholesterol monohydrate is raised to ∼95 °C (*32*, *33*). We have measured the DSC of equimolar mixtures of cholesterol and several forms of phosphatidylcholine in either the presence or absence of *N*-acetyl-LWYIK-amide. In the absence of peptide, only a trace amount of a transition corresponding to cholesterol crystals can be detected with an equimolar mixture of

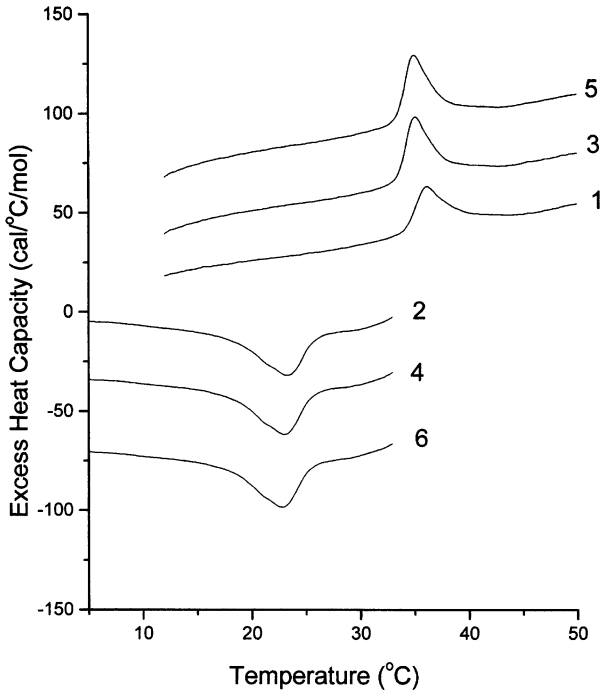

FIGURE 2: Differential scanning calorimetry of POPC/cholesterol (1:1) with 10 mol % *N*-acetyl-LWYIK-amide. Scan rate was 2 K/min. Lipid concentration was 2.5 mg/mL in 20 mM PIPES, 1 mM EDTA, and 150 mM NaCl with 0.002% NaN_3, pH 7.40. Sequential heating and cooling scans were perfomed between 0 and 50 °C. Numbers are the order in which the scans were carried out, with scans 1, 3, and 5 being heating scans, each of which was followed by one of the cooling scans 2, 4, or 6. Scans were displaced along the *y*-axis for clarity of presentation.

cholesterol and SOPC (Figure 3). Significant amounts of cholesterol crystals are formed in SOPC only at a cholesterol mole fraction of 0.7 or higher (*27*). With equimolar mixtures of cholesterol and any of the other PCs used, no transition corresponding to cholesterol crystals is observed (not presented). A broad low temperature (below 10 °C) transition, corresponding to the chain melting transition of the phospholipid, can be observed on heating or cooling in samples with an equimolar content of cholesterol and POPC or SOPC. Upon the addition of 10 mol % acetyl-LWYIK-amide there is the appearance of a transition at ∼37 °C on heating and at 22 °C on cooling, at a scan rate of 2 K/min with POPC (Figure 2), as well as with DOPC (not shown) and SOPC (Figure 3). These temperatures correspond to the polymorphic transition of anhydrous cholesterol in both heating and cooling at this scan rate (*34*). The transitions are reproducible in sequential scans provided the sample is not heated above 50 °C (Figures 2 and 3). If the sample is heated to 100 °C, the first heating scan shows the polymorphic transition of anhydrous cholesterol but no transition for the dehydration of cholesterol monohydrate. There is about 10% loss of enthalpy for the polymorphic transition of anhydrous cholesterol on each subsequent heating and cooling scan upon heating to 100 °C, but no loss upon heating to only 50 °C. The magnitude of the peak for the polymorphic transition of cholesterol for samples not heated above 50 °C is 6 ± 2, 140 ± 10, and 80 ± 5 cal/mol of cholesterol for the mixtures with DOPC, POPC, and SOPC, respectively, containing 10 mol % *N*-acetyl-LWYIK-amide. These transitions are not present to a significant extent in the absence of peptide. For equimolar mixtures of SOPC and cholesterol, the enthalpy

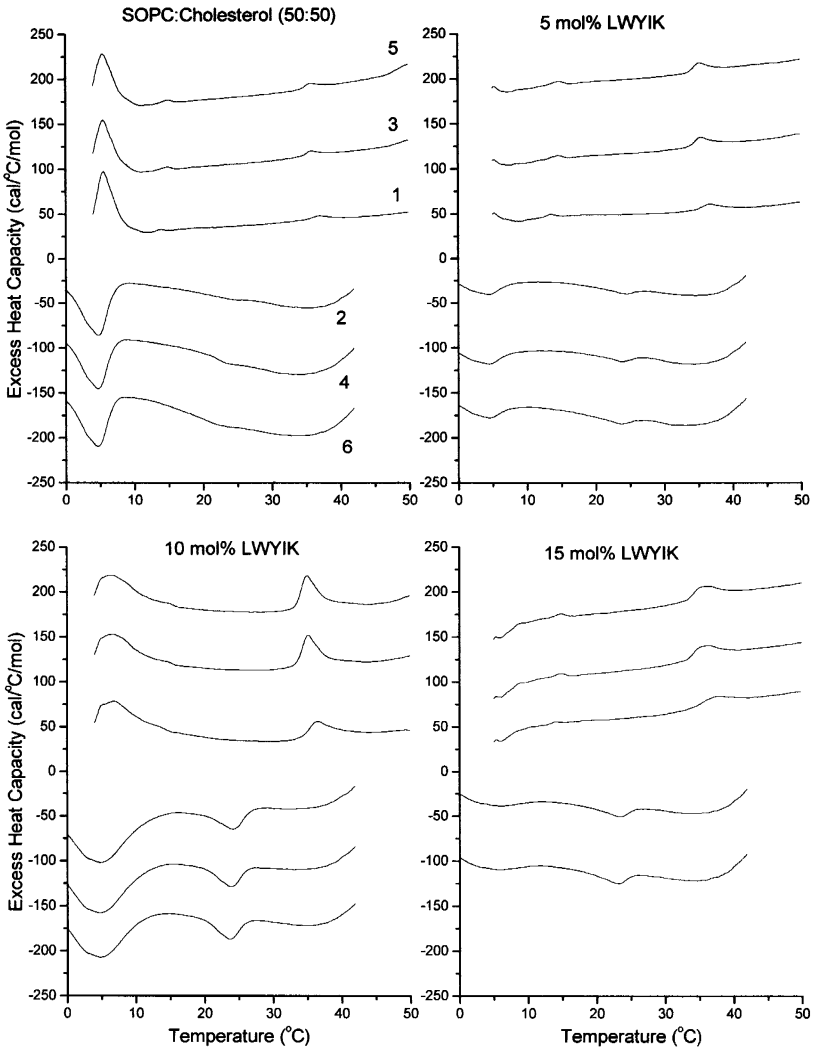

FIGURE 3: Differential scanning calorimetry of SOPC/cholesterol (1:1) with 0, 5, 10, or 15 mol % *N*-acetyl-LWYIK-amide. Conditions were as described for Figure 2. Scan numbers are shown only for the pure lipid, but the same order is used for other panels in this figure as well as for Figures 4 and 5.

of the polymorphic crystalline transition of cholesterol increases from 25 to 80 cal/mol of cholesterol in going from 5 to 10 mol % peptide. However, at 15 mol % peptide this transition becomes broader and the measured enthalpy is reduced to 60 cal/mol of cholesterol. From the known enthalpy of these transitions (*35*), we can calculate that the presence of 10 mol % peptide results in 0.6%, 15%, and 9% of the cholesterol forming crystals at an equimolar ratio of cholesterol with DOPC, POPC, or SOPC, respectively. The results demonstrate that the peptide has a large effect in promoting the segregation of cholesterol in mixtures with phosphatidylcholine.

For comparison, we measured the DSC of an equimolar mixture of POPC and cholesterol in the presence of 10 mol % of the peptide *N*-acetyl-KYWFYR-amide. No crystalline cholesterol phase transitions were observed with these mixtures, whether the sample was heated to 50 or to 100 °C. This indicates that, unlike *N*-acetyl-LWYIK-amide, the peptide *N*-acetyl-KYWFYR-amide does not promote the clustering of cholesterol into domains where it passes its solubility limit in the membrane.

Among the forms of PC used in this study, SOPC is the only one with a phase transition temperature above 0 °C. We have studied the effect of *N*-acetyl-LWYIK-amide on the gel to liquid crystalline transition of this lipid in the presence of different mole fractions of cholesterol as well as on the formation of cholesterol crystallites. At cholesterol mole fractions of 0.3 (Figure 4) or 0.4 (Figure 5), increasing amounts of peptide cause a significant increase in the enthalpy of the chain melting transition of the phospholipid. Although it is not possible to extend the scan below 0 °C, we can estimate the enthalpy of the chain melting transition in the presence of cholesterol and peptide from the cooling scans (Table 1).

In contrast with the marked effects of the peptide on the organization of mixtures of cholesterol with SOPC, the peptide has very little effect on the chain melting transition of pure SOPC. The DSC of SOPC alone, at a scan rate of 2 K/min, exhibits a thermal transition at 6.1 °C on heating and 5.5 °C on cooling, with a transition enthalpy of 4 kcal/mol. In the presence of 10 mol % *N*-acetyl-LWYIK-amide the values are 5.9 °C on heating and 5.3 °C on cooling, with a transition enthalpy of 4 kcal/mol (not shown).

Partitioning of N-Acetyl-LWYIK-amide between Membrane and Aqueous Phases. In the DSC experiments described above, the peptide was added in organic solvent to form a component of the lipid film that was subsequently hydrated. If a pure lipid film was hydrated with an aqueous solution

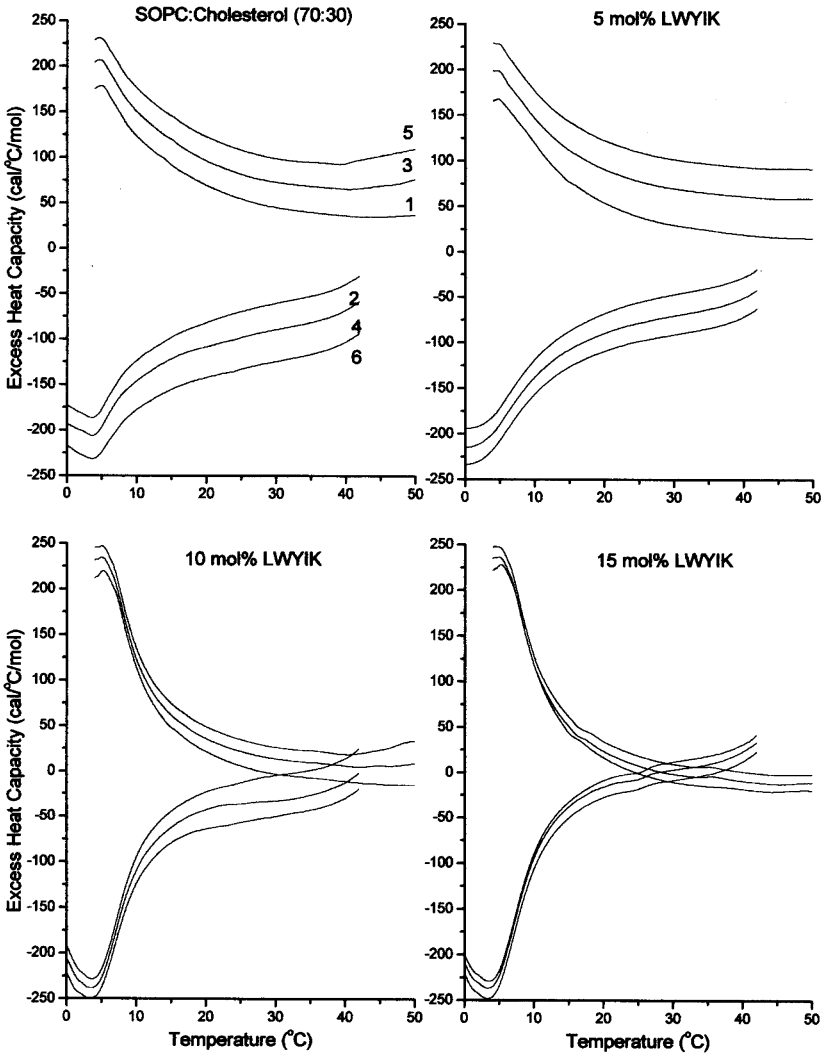

FIGURE 4: Differential scanning calorimetry of SOPC/cholesterol (7:3) with 0, 5, 10 or 15 mol % *N*-acetyl-LWYIK-amide. Conditions were as described for Figure 2.

of the peptide, little or no enthalpy corresponding to the formation of cholesterol crystallites is observed. Also, as mentioned above, if the peptide−lipid mixture was heated to 100 °C, the enthalpy of the peak corresponding to crystalline cholesterol decreased. These observations indicate that there are kinetic effects altering the partitioning of the peptide between water and the membrane.

We determined the rate at which *N*-acetyl-LWYIK-amide dissociated from liposomes of POPC either containing or not containing 0.5 mol fraction cholesterol. MLVs were formed from a lipid film of POPC, with or without cholesterol, also containing 10 mol % *N*-acetyl-LWYIK-amide and 5 mol % DNS-PE. Controls performed in the absence of peptide gave several fold lower fluorescence emission intensity from the DNS group, indicating that Trp residue of the peptide underwent resonance energy transfer to the DNS group. However, this enhanced fluorescence was gradually lost as a function of time. The loss was somewhat more rapid from membranes not containing cholesterol (Figure 6).

Although the peptide partitioning between water and membrane is slow to equilibrate, the replicate scans in the DSC show good reproducibility. We determined the fraction of peptide that was bound to the membrane in the samples taken after three heating and three cooling scans between 0 and 50 °C. This was done simply by centrifuging these samples and determining the concentration of peptide in the supernatant. Although there is some dissociation of peptide, the major fraction of the peptide is still bound to the membrane (Figure 7). A greater fraction is bound to the membrane containing cholesterol. The amount of peptide that is membrane-bound after equilibration is greater than that found in the resonance energy transfer assay (Figure 6), simply because the concentrations of peptide and lipid are greater in this case. Thus, the *N*-acetyl-LWYIK-amide binds to membranes in both the presence and absence of cholesterol, but cholesterol enhances the interaction of this peptide with the membrane.

^{1}H MAS NMR. Static ^{31}P NMR powder patterns demonstrated that all of the samples used for MAS studies were in bilayer arrangement (not shown). Two-dimensional (2-D) ^{1}H MAS NOESY spectra were recorded at 25 °C for five samples: POPC, POPC/cholesterol (1:1), POPC with 10 mol % *N*-acetyl-LWYIK-amide, POPC/cholesterol (1:1) with 10 mol % *N*-acetyl-LWYIK-amide, and POPC/cholesterol (1:1) with 10 mol % *N*-acetyl-KYWFYR-amide. No resonances assignable to cholesterol could be detected either with or without the peptide, in agreement with earlier observations

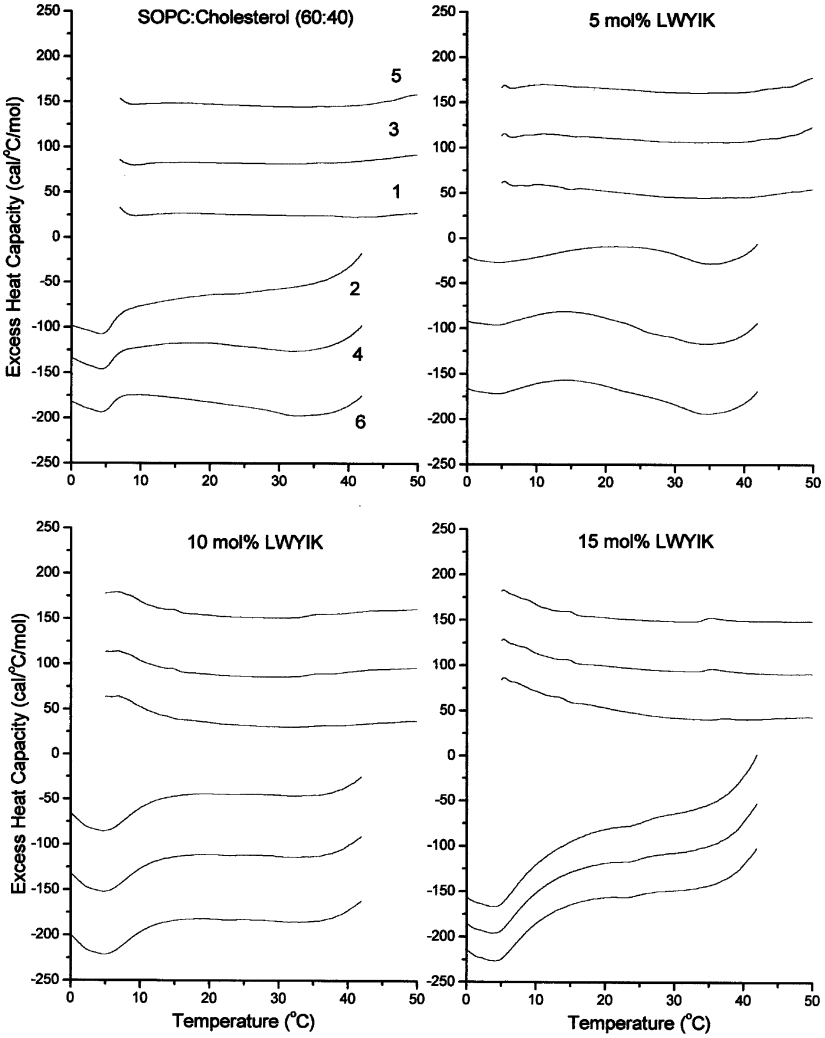

FIGURE 5: Differential scanning calorimetry of SOPC/cholesterol (6:4) with 0, 5, 10 or 15 mol % *N*-acetyl-LWYIK-amide. Conditions were as described for Figure 2.

Table 1: Estimated Enthalpy of the Gel to Liquid-Crystalline Phase Transition of SOPC in the Presence of Cholesterol and *N*-Acetyl-LWKYIK

mol % cholesterol	mol % *N*-acetyl-LWYIK-amide	ΔH (kcal/mol of SOPC)
30	0	0.5
30	5	1.0
30	10	1.1
30	15	1.2
40	0	0.1
40	5	0.1
40	10	0.3
40	15	0.5

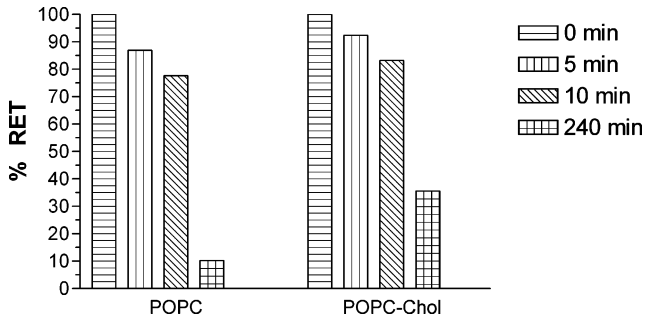

FIGURE 6: Dissociation of *N*-acetyl-LWYIK-amide from liposomes of POPC/cholesterol (1:1) containing 5 mol % DNS-PE and 10 mol % peptide. Lipid concentration was 300 μM; temperature was 25 °C. Peptide dissociation was monitored by the decreased DNS fluorescence emission as a result of loss of energy transfer from the Trp of the peptide.

(*23*). The peptide is in relatively low concentration and many of its resonances would not be well resolved from those of the lipid. The only resonances that are clearly assignable to the peptide are those of the aromatic protons, in the region 6−8 ppm. The presence of these signals indicates that a large fraction of the peptide remains in the sample. This is expected because the high concentrations used for NMR would cause the peptide to partition into the membrane and the sample was transferred to the NMR rotor soon after preparation, not allowing time for the peptide to dissociate. Peaks assignable to aromatic protons include the resonance at 7.5 ppm from Trp $H^{\zeta 3}$; those at 7.1 and 7.0 ppm that are likely to have contributions from both Tyr and Trp; and the one at 6.8 ppm from Tyr $H^{\epsilon 1/\epsilon 2}$; in addition, KYWFYR has a resonance from Phe at 7.3 ppm (*25*). We have focused on the relative strength of the NOE interactions between these aromatic amino acid side chains and other atoms. Stronger NOE interactions between two atoms are a measure of their closer approach. These are observed as peaks in the 2-D NOESY spectra. Slices of the NOESY at the resonance position of the aromatic protons are shown for the spectra of *N*-acetyl-LWYIK-amide with POPC or with equimolar POPC and

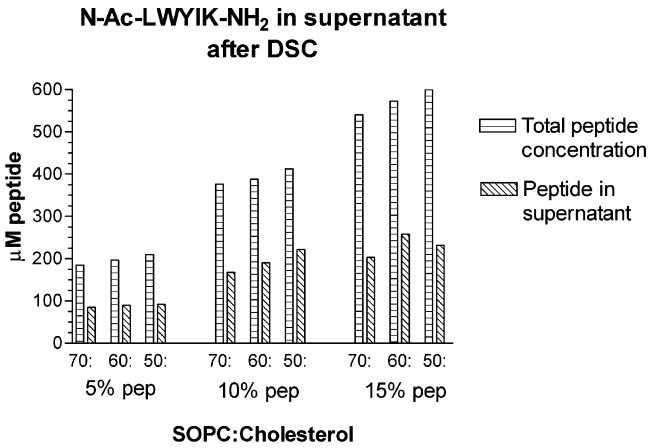

FIGURE 7: Binding of *N*-acetyl-LWYIK-amide to MLV of SOPC with 0.3, 0.4, or 0.5 mol fraction cholesterol, each containing 5, 10, and 15 mol % peptide, after the series of DSC runs shown in Figures 3−5. Error bars are SEM of experiments repeated three times.

cholesterol with a delay time of 50 ms (Figure 8) as well as for 300 ms (Figure 9). The longer delay times result in larger NOEs by allowing more complete energy transfer through dipolar interactions. However, longer delay times can also allow NOE effects to be observed between two groups that are not physically close to each other as a result of spin diffusion. It is likely, however, that at least with a 50 ms delay time, spin diffusion does not contribute greatly to the observed dipolar interactions (*36*). In general, the number and intensity of the cross-peaks between the peptide aromatic protons and the acyl chain protons are greater when cholesterol is incorporated into the membrane. This can be seen in virtually all of the slices but is particularly clear upon comparison of the signal from the terminal methyl group of the acyl chains, which is absent for the slices at 6.82, 6.98, and 7.13 ppm in the absence of cholesterol but present in those from the sample with cholesterol, with a mixing time of 50 ms (Figure 8).

We have also measured the cross-peaks between the quaternary ammonium methyl protons of the lipid headgroup, at 3.28 ppm, and the aromatic protons of the peptide *N*-acetyl-LWYIK-amide. The segment of the slice at 3.28 ppm covering the aromatic resonances exhibits peaks for the sample in the absence of cholesterol but not for the one containing cholesterol (Figure 10). This is opposite to what we showed for the peptide interactions with the aliphatic protons of the lipid. Thus the peptide interacts with the membrane both in the presence and absence of cholesterol, but a larger fraction of the peptide is at the bilayer interface in the absence of cholesterol, rather than penetrating into the bilayer. The depth of penetration of the aromatic groups into the bilayer is greater in the presence of cholesterol.

The sign of the NOESY peak is indicative of the motional properties of the groups giving rise to the cross-peaks, and a negative NOESY peak corresponds to rapid motion. Most of the peaks observed in the NOESY spectrum are positive in sign, as expected for the high molecular weight aggregate of a membrane. However, with a delay time of 300 ms (Figure 9), there are several negative peaks observed in the sample without cholesterol, particularly in the slice at 6.82 ppm (Figure 9). We interpret this result as indicating that the peptide can exchange between a membrane-bound form and a water-soluble form. We suggest that the rate of exchange between these two environments is slow compared with the shorter mixing time of 50 ms and that the equilibrium is toward most of the peptide being in the membrane-bound form, thus giving rise to positive peaks in the NOESY spectrum. However, at the longer mixing time, exchange between free and membrane-bound peptide can take place and the free peptide has rapid motions that can randomize the orientation of the peptide with respect to the

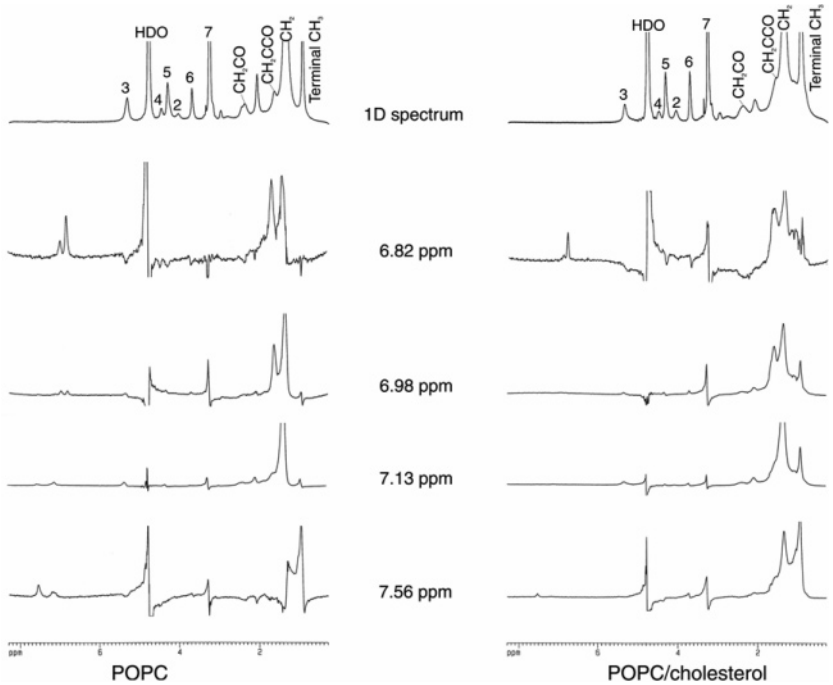

FIGURE 8: One-dimensional slices from the MAS ^{1}H NOESY spectrum at the chemical shifts of the aromatic protons with a mixing time of 50 ms. Spectra are taken from samples of POPC or POPC/cholesterol (1:1), each containing 10 mol % acetyl-LWYIK-amide. Top spectra are conventional 1-D proton spectra of the samples. Resonance assignments are indicated on the top spectrum according to the numbering system given in Figure 1.

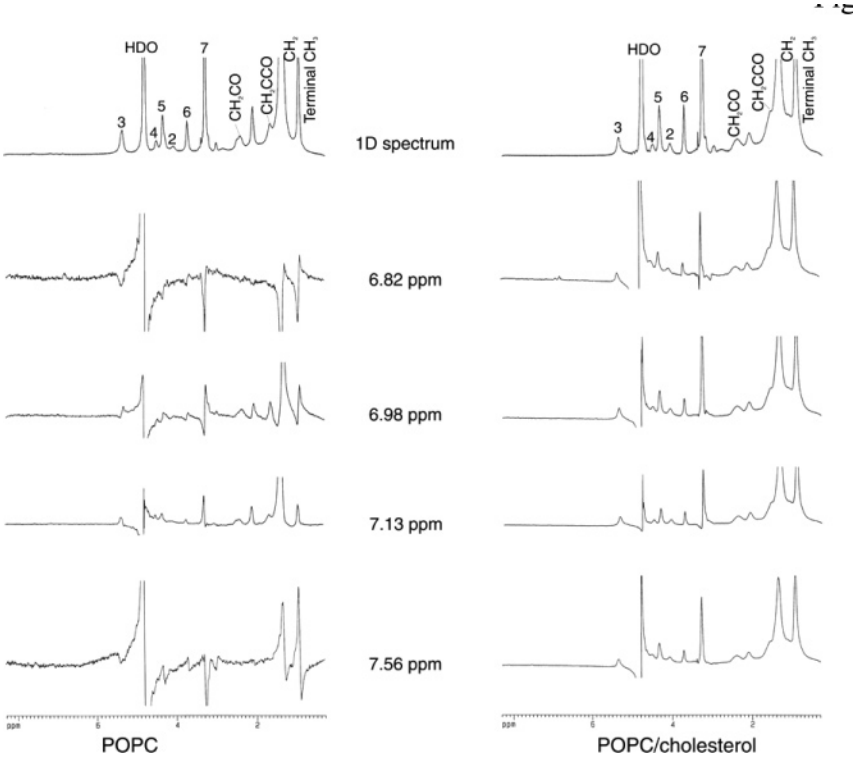

FIGURE 9: One-dimensional slices from the MAS ^{1}H NOESY spectrum at the chemical shifts of the aromatic protons with a mixing time of 300 ms. Conditions are as described for Figure 8.

lipid. Hence, millisecond slow exchange processes can determine how effectively the nanosecond motions that occur in the free peptide can reverse the sign of the NOE. This does not happen in the sample with cholesterol because there is less free peptide in this case.

We have also compared the chemical shifts of the observed resonances in the samples of POPC, POPC/cholesterol (1:1), POPC with 10 mol % *N*-acetyl-LWYIK-amide, and POPC/cholesterol with 10 mol % *N*-acetyl-LWYIK-amide (1:1) (Table 2). Changes in chemical shift of a group can occur because of a change in environment or because of ring current effects from the aromatic groups. The addition of cholesterol results in a small change of the chemical shift, of 0.05 ppm or less, of certain resonances, suggesting a small change of environment of some of the groups of the lipid. However, addition of 10 mol % of the *N*-acetyl-LWYIK-amide has essentially no effect on any of the chemical shifts (0.01 ppm or less), in samples either with or without cholesterol, indicating that the peptide is not interacting strongly with the phospholipid component of the membrane.

The NOESY spectra of an equimolar mixture of POPC and cholesterol containing 10 mol % *N*-acetyl-KYWFYR-amide were measured with the two mixing times of 50 and 300 ms (Figure 11). Qualitatively there are many similarities between the NOESY spectrum with this peptide and with the *N*-acetyl-LWYIK-amide, except for the slices at 6.8 ppm, corresponding to the resonances of the Tyr $H^{\epsilon 1/\epsilon 2}$. The cross-peaks between this group and the hydrocarbon resonances from the lipid are much weaker in the case of the *N*-acetyl-KYWFYR-amide. This is the case for both peaks corresponding to Tyr, with chemical shifts of 6.79 ppm (likely the Tyr near the carboxyl terminus) and 6.84. This indicates that a portion of the *N*-acetyl-KYWFYR-amide is less inserted into the membrane than any of the aromatic groups

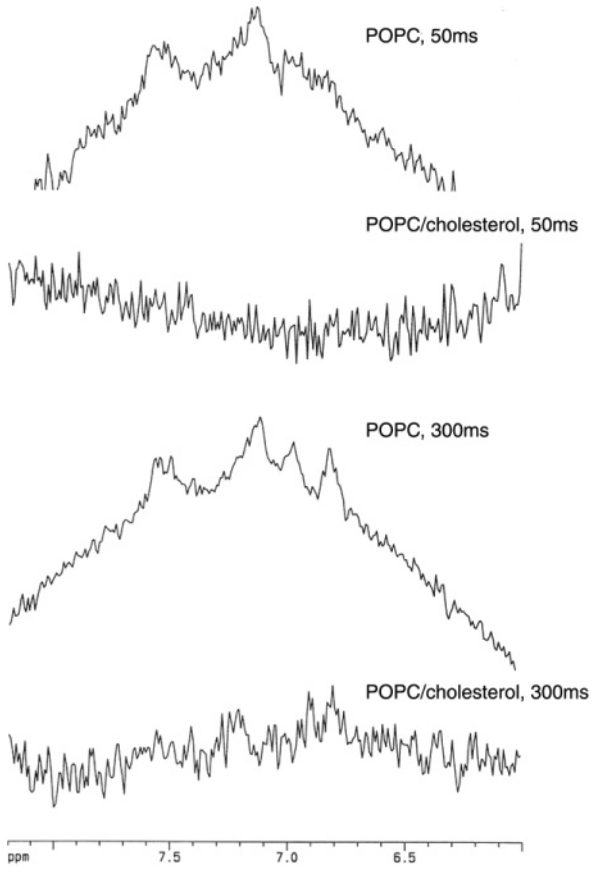

FIGURE 10: Slice from the MAS ^{1}H NOESY at 3.28 ppm, corresponding to the resonance of the quaternary ammonium group. The region of the aromatic resonances is shown for samples of POPC or POPC/cholesterol (1:1), each containing 10 mol % acetyl-LWYIK-amide. Spectra with mixing times of 50 and 300 ms are shown.

Table 2: ^{1}H Chemical Shift of Lipid Resonances without and with *N*-Acetyl-LWYIK-amide

	sample			
resonance[a]	POPC	POPC/ cholesterol (1:1)	POPC + 10% *N*-acetyl-LWYIK-amide	POPC/ cholesterol (1:1) + 10% *N*-acetyl-LWYIK-amide
glycerol C2 (3)	5.329	5.374	5.342	5.376
H_2O	4.800	4.801	4.798	4.805
glycerol C3 (4)	4.476	4.521	4.488	4.526
choline α (5)	4.336	4.354	4.333	4.357
glycerol C1 (2)	4.055	4.082	4.062	4.090
choline β (6)	3.739	3.746	3.729	3.746
quaternary CH_3 (7)	3.296	3.301	3.287	3.299
CH_2CO	2.387	2.413	2.393	2.422
CH_2CCO	1.656	*b*	1.653	*b*
CH_2	1.347	1.373	1.353	1.372
terminal CH_3	0.944	0.953	0.951	0.952

[a] Numbers in parentheses correspond to numbering shown in Figure 1. [b] Resonance not well resolved.

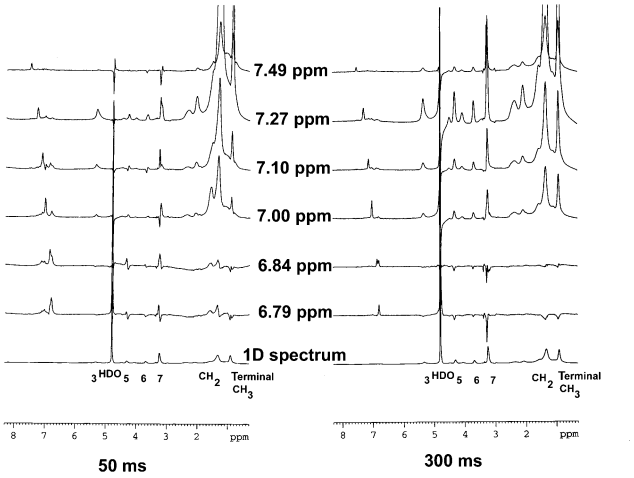

FIGURE 11: One-dimensional slices from the MAS ^{1}H NOESY spectrum at the chemical shifts of the aromatic protons with a mixing time of 50 ms (left) and 300 ms (right). Spectra are taken from a sample of POPC/cholesterol (1:1) containing 10 mol % acetyl-KYWFYR-amide. Bottom spectra are conventional 1-D proton spectra of the sample.

of *N*-acetyl-LWYIK-amide. Thus, although aromatic groups tend to partition close to the membrane interface, the exact position of these residues in the bilayer is not identical for all systems but is influenced by the nature of the lipid and the surrounding amino acid residues. In contrast to the resonances from the two Tyr residues, the one at 7.27 ppm from Phe exhibits particularly large cross-peaks with the aliphatic resonances of the lipid. Thus, even in these relatively simple peptide−lipid systems, it would be an oversimplification to consider all the aromatic amino acid side chains to be present at a similar position near the membrane interface.

As with *N*-acetyl-LWYIK-amide, the cholesterol proton resonances are not detectable with *N*-acetyl-KYWFYR-amide in an equimolar mixture of POPC and cholesterol. However, in the case of *N*-acetyl-KYWFYR-amide, the peptide induces small but significant changes in the chemical shift of the resonances of POPC (Table 3).

^{13}C MAS NMR Studies. Since cholesterol resonances are not observed in the ^{1}H MAS NMR spectra, we have further

Table 3: ^{1}H Chemical Shift Differences of Lipid Resonances with *N*-Acetyl-KYWFYR-amide

resonance	chemical shift difference[a]
glycerol C2 (3)	0.04
H_2O	0.00
glycerol C3 (4)	0.06
choline α (5)	0.05
glycerol C1 (2)	0.03
choline β (6)	0.06
quaternary CH_3 (7)	0.06
CH_2CO	0.06
CH_2	0.05
terminal CH_3	0.04

[a] Chemical shift differences are in parts per milliion between POPC/cholesterol (1:1) and POPC/cholesterol (1:1) + 10% *N*-acetyl-KYWFYR-amide.

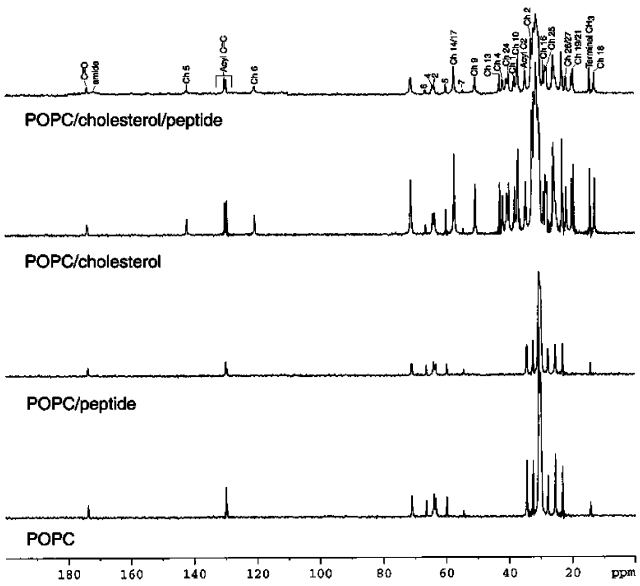

FIGURE 12: ^{13}C CP/MAS NMR of POPC, POPC with 10 mol % *N*-acetyl-LWYIK-amide, POPC/cholesterol (1:1), and POPC/cholesterol with 10 mol % *N*-acetyl-LWYIK-amide (1:1). Measurements were made at 75.48 MHz with sample spinning at 5 kHz at 25 °C and a contact time of 1 ms. Resonance assignments are indicated on the top spectrum according to the numbering system given in Figure 1, with resonances from cholesterol being preceded by the letters Ch.

investigated the system by both ^{13}C CP/MAS NMR (Figure 12) and direct polarization ^{13}C MAS NMR (Figure 13). The former is sensitive to the more solidlike domains, while the later should detect all signals, providing that the delay time is sufficiently long for spin relaxation. The resonance for the C18 of cholesterol is observed at 12.8 ppm in both CP/MAS (Figure 12) and in direct polarization (Figure 13), indicative of cholesterol dissolved in the membrane (*37*). No peaks corresponding to crystalline cholesterol are observed, although a small amount of anhydrous crystalline cholesterol was observed by DSC in samples containing 10 mol % *N*-acetyl-LWYIK-amide. The CP/MAS (Figure 12) and the direct polarization spectra (Figure 13) show some differences. In particular, the resonance for the quaternary ammonium group (resonance 7) is barely observable by CP/MAS, but it is the largest peak in the spectra obtained by direct polarization. This indicates that this group is relatively mobile and therefore not observable in CP/MAS, while essentially all of the other groups are relatively immobile and their motional properties are not drastically affected by the presence of the

Table 4: ^{13}C Chemical Shift Differences of Lipid Resonances[a]

assignment[b]	chemical shift (ppm)	POPC ± *N*-acetyl-LWYIK-amide	POPC/cholesterol (1:1) ± *N*-acetyl-LWYIK-amide	POPC/cholesterol (1:1) ± *N*-acetyl-KYWFYR-amide	POPC ± cholesterol
acyl C═O	174	0.016	0.055	0.175	−0.200
cholesterol C5	142		0.133	0.374	
acyl C═C	130.1	0.017	0.051	0.113	−0.095
acyl C═C	129.6	0.012	0.031	0.079	0.024
cholesterol C6	121		0.070	0.061	
glycerol C2 (3)	71	0.020	0.136	0.225	
choline β (6)	66	0.019	0.034	0.118	−0.042
glycerol C3 (4)	64	−0.040	0.083	0.093	−0.205
glycerol C1 (2)	63	0.012	0.021	0.122	−0.161
choline α (5)	60	0.025	0.080	0.126	−0.091
cholesterol C14/17	57		0.032	0.113	
quaternary CH_3 (7)	54	0.015	0.078	0.136	−0.057
cholesterol C9	51		0.038	0.085	
cholesterol C13	43		0.037	0.109	
cholesterol C4	42		0.084	ND[c]	
cholesterol C24	40		0.042	0.111	
cholesterol C1	38		0.032	0.446	
cholesterol C10	37		0.046	0.102	
acyl C2	35	0.005	0.066	0.140	−0.275
cholesterol C2	31		0.160	0.124	
cholesterol C16	29		0.042	−0.311	
cholesterol C25	28		0.020	−0.203	
cholesterol C26/27	23		0.037	−0.073	
cholesterol C19/21	20		0.042	0.136	
acyl terminal methyl	14	0.024	0.030	0.081	−0.002
cholesterol C18	12.8		0.062	0.188	

[a] Data show the chemical shift differences in parts per million: (column 3) between POPC and POPC + 10% *N*-acetyl-LWYIK-amide; (column 4) between POPC:cholesterol (1:1) and POPC:cholesterol (1:1) + 10% *N*-acetyl-LWYIK-amide; (column 5) between POPC and POPC:cholesterol (1:1). [b] Numbers in parentheses correspond to numbering shown in Figure 1. [c] ND, not determined because of poor resolution of the peak.

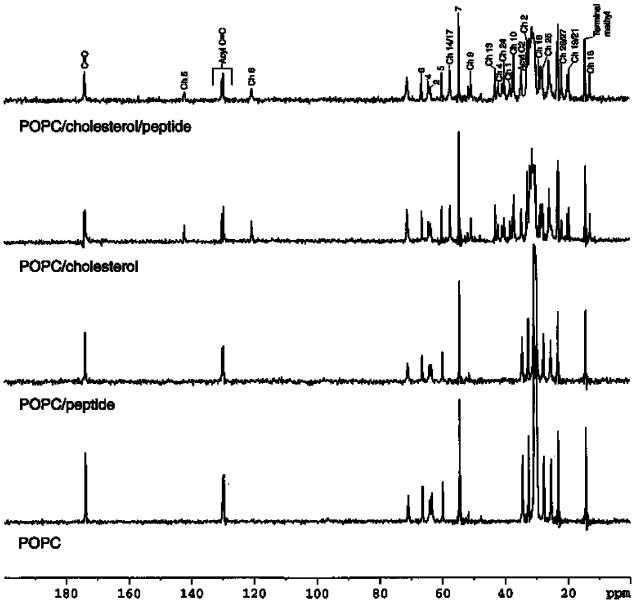

FIGURE 13: Direct polarization spectra from the same samples used for Figure 12. Measurements were made at 75.48 MHz with sample spinning at 5 kHz at 25 °C and a delay time of 5 s. Resonance assignments are indicated on the top spectrum according to the numbering system given in Figure 1, with resonances from cholesterol being preceded by the letters Ch.

peptide. In the CP/MAS spectra of POPC/cholesterol/peptide a broad peak for the amide carbonyl groups of the peptide can be observed at about 170 ppm (Figure 12). However, it is not seen in the spectrum without cholesterol, indicating that the motional properties of the peptide are markedly altered by cholesterol. A more detailed analysis with a series of mixing times would be required to further study this difference, which was not pursued because of the weak intensity of this peak.

We have compared the chemical shifts of the ^{13}C resonances with and without 10 mol % either *N*-acetyl-LWYIK-amide or *N*-acetyl-KYWFYR-amide (Table 4). Values obtained by CP/MAS and direct polarization were averaged when the signal was observed by both methods. In general, the changes in the peak position of lipid resonances caused by the peptide were relatively small, particularly for *N*-acetyl-LWYIK-amide in the absence of cholesterol. The largest change caused by the addition of *N*-acetyl-LWYIK-amide to the sample without cholesterol is for the C3 position of glycerol. This resonance is also one that is strongly shifted by the addition of cholesterol. The C3 of glycerol is at the membrane interface. It is shifted downfield by cholesterol, indicating that the environment around this group is becoming less hydrophobic. Interestingly, the further shift caused by the addition of the peptide is in opposite directions with and without cholesterol. The presence of the peptide causes the sequestering of cholesterol, decreasing the effect of cholesterol on the chemical shift of glycerol C3 in the presence of the peptide. The results suggest that the peptide increases the tightness of packing at the interface for membranes with cholesterol, but the peptide increases interfacial polarity for membranes not containing cholesterol. The membrane interface is complex and its polarity is sensitive to distance (*38*). *N*-Acetyl-LWYIK-amide-induced shifts of about 0.08 ppm in the ^{13}C chemical shifts of the glycerol C3, the choline C^{α}, and the quaternary methyl groups (Table 4), although the proton resonances of these groups do not change (Table 2). However, the 1-D ^{1}H NMR

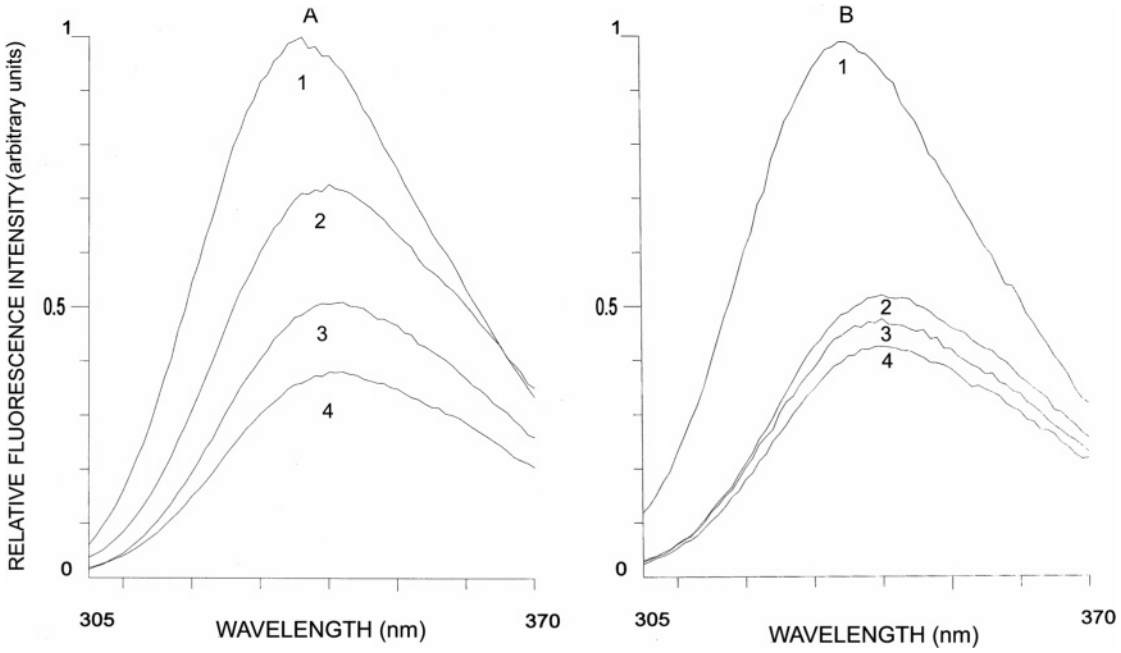

FIGURE 14: Fluorescence emission of *N*-acetyl-LWYIK-amide (A) and acetyl-KYWFYR-amide (B). Excitation wavelength was 280 nm. Spectra are for a solution of the peptide in methanol (curve 1) or in water (curve 2), the peptide mixed with sonicated liposomes of POPC at a 1:1 peptide:lipid ratio (curve 3), or the peptide mixed with sonicated liposomes of POPC:cholesterol (1:1) at a 1:1 peptide:phospholipid ratio (curve 4). All samples contained 150 μM peptide. The spectra are plotted relative to the maximum emission intensity in methanol as 1.

spectra reveal that the peaks for these atoms have high-field shoulders. We suggest that these shoulders represent the fraction of the lipid that is interacting more strongly with the peptide. In the case of the ^{13}C spectra, the longer relaxation time allows for exchange processes to average these environments, giving rise to a change in the chemical shift. The effect is relatively small, with the change being less than 0.1 ppm, but the results are not inconsistent with the proton data in which even these small shifts are not observed. In addition, ^{13}C chemical shifts span a wider range than do those of ^{1}H and can therefore be more sensitive to changes in environment. Large changes are observed in some of the resonances from cholesterol. The cholesterol C5 and C2 resonances in the POPC/cholesterol samples were shifted 0.13 and 0.16 ppm, respectively, by the addition of *N*-acetyl-LWYIK-amide. We suggest that these larger chemical shift changes are a consequence of ring current effects. Aromatic groups will cause a downfield shift of groups at the edges of the ring but an upfield shift for groups that are above or below the ring. Both the C2 and C5 carbons of cholesterol are in the A ring and are shifted upfield (to lower frequencies) by the peptide. This suggests that one or more of the aromatic side chains of the peptide are stacked face to face with the A ring of cholesterol. Other atoms in the A ring of cholesterol are C4, which is shifted 0.08 ppm, and C1 and C3, which is not well resolved from other signals. The direction and magnitude of the shifts we observe for C5 and C2 are comparable to those observed with the WALP peptides and lipid at a similar peptide:lipid ratio of 1:10 (*39*). Indole and its derivates at a higher mole fractions cause a larger change in the chemical shift (*40*). Our results then indicate that within the bilayer the *N*-acetyl-LWYIK-amide interacts more strongly with cholesterol than it does with POPC. This is in contrast to the behavior of *N*-acetyl-KYWFYR-amide, which induces significant chemical shift changes for both POPC (Tables 3 and 4) and cholesterol (Table 4). However, both peptides show a large effect on the ^{13}C chemical shift of cholesterol C5 (Table 4).

Tryptophan Fluorescence Emission. The fluorescence emission spectra of the Trp residues of *N*-acetyl-LWYIK-amide and of *N*-acetyl-KYWFYR-amide have maxima at 340 nm for the peptide dissolved in water as well as in the presence of SUVs of POPC or POPC with 0.5 mol fraction cholesterol (Figure 14). These emission spectra are not very different from that of the peptide in methanol, which has a maximum at 336 nm. This indicates that the Trp of this peptide in water is blue-shifted compared with the usual emission wavelength for Trp in water of ~350 nm. The polarity of the environment does not change much from water when the peptide is mixed with liposomes of either POPC or POPC:cholesterol (1:1). However, for *N*-acetyl-LWYIK-amide the emission intensity is significantly reduced in the presence of the liposomes, indicating that the peptide is interacting with the lipid and that this interaction is different in the presence and absence of cholesterol. For *N*-acetyl-LWYIK-amide, the maximum intensity of tryptophan in cholesterol-containing liposomes is half that of liposomes without cholesterol (Figure 14). In the case of *N*-acetyl-KYWFYR-amide there is less effect of the lipid on the emission intensity and less change when cholesterol is added to the membrane (Figure 14).

Upon comparison of the emission spectra of acetyl-LWYIK-amide in the various conditions with excitation wavelengths of 280 and 295 nm, there is no indication of any peak at ~300 nm, corresponding to emission from Tyr. It is likely that resonance energy transfer from Tyr to Trp in this small peptide contributes to the low quantum yield of Tyr.

DISCUSSION

A consensus sequence that is found in a group of proteins that sequester to cholesterol-rich regions of membranes

has the pattern -L/V-(X)(1−5)-Y-(X)(1−5)-R/K-, in which (X)(1−5) represents 1−5 residues of any amino acid (*12*). The HIV-1 fusion protein gp41 has a segment, LWYIK, consistent with this consensus sequence that is responsible for this protein sequestering into cholesterol-rich domains. The results of this paper indicate that this peptide segment facilitates the movement of proteins into cholesterol-rich domains because of the nature of its interactions with lipids. This supports an earlier suggestion that the membrane-proximal region might establish direct interactions with cholesterol (*13*). Furthermore, the preferential interaction of this segment with cholesterol also results in the stabilization of cholesterol-rich domains. In the case of the gp41 protein of HIV, which contains the LWYIK sequence, these cholesterol-rich domains also have other characteristics that operationally classify them as rafts (*15*). In contrast, the peptide segment KYWFYR, although part of a longer sequence that targets caveolin-1 to cholesterol-rich caveolae, itself is not sufficient for targeting to cholesterol-rich domains (*19*), nor does it fulfill the consensus sequence suggested by Li and Papadopoulos (*12*). We find that, in contrast to *N*-acetyl-LWYIK-amide, the peptide *N*-acetyl-KYWFYR-amide shows no preferential interaction with cholesterol as indicated by the fact that it does not promote the formation of cholesterol crystallites and it affects the NMR resonances of both POPC and cholesterol to a comparable extent.

Addition of *N*-acetyl-LWYIK-amide to bilayers of PC and cholesterol results in the appearance of calorimetric transitions corresponding to the formation of cholesterol crystallites (Figures 2 and 3). A similar segregation of cholesterol crystals in mixtures with SOPC was previously observed with the protein NAP-22 (*41*), isolated from the raft fraction of neurons. NAP-22 binds to liposomes containing high mole fractions of cholesterol, but not to liposomes composed only of phosphatidylcholine. However, the molecular basis for this phenomenon involves cholesterol-dependent dissociation of protein oligomers (*42*). In the case of *N*-acetyl-LWYIK-amide there is preferential interaction with cholesterol, as indicated by the peptide-promoted formation of cholesterol crystals at high cholesterol mole fractions as well as by the partial depletion of cholesterol from a membrane domain, as indicated by the increase in the enthalpy of the phospholipid phase transition. In addition, NMR spectra indicate that this peptide has a greater effect on the resonances of cholesterol than on the phospholipids. Nevertheless, *N*-acetyl-LWYIK-amide shows little preferential binding to liposomes containing cholesterol (Figure 7). The peptide is slow to equilibrate between aqueous and membrane phases (Figure 6) and the final partitioning of the peptide depends on its concentration. At a low concentration of 30 μM peptide (Figure 6), most of the peptide dissociates from the membrane, but at a higher concentration (Figure 7) and especially at the very high concentrations of >100 mM used for NMR, most of the peptide will remain associated with the membrane.

Our DSC studies demonstrate that *N*-acetyl-LWYIK-amide can facilitate the formation of cholesterol-rich domains in membranes. This has also been observed with NAP-22 (*43*). In model systems it is known that lipid mixtures of sphingomyelin, cholesterol, and phosphatidylcholine will spontaneously form cholesterol-rich domains (*44*, *45*). This mechanism is currently thought to drive the formation of raft domains in biological membranes. However, our findings indicate that proteins will also influence this process. This may be of particular importance for the formation of cholesterol-rich domains on the cytoplasmic leaflet, where sphingomyelin is not as abundant as it is in the external leaflet. The interaction that occurs between *N*-acetyl-LWYIK-amide is not a specific stoichiometric complex since the extent of formation of the cholesterol crystallites depends on the nature of the PC and the maximal interactions are observed at high cholesterol to peptide molar ratios. This is also the case for NAP-22 (*46*). A longer peptide containing the LWYIK sequence has been shown to penetrate more deeply into membranes containing cholesterol both by the promotion of liposome content leakage and by surface pressure measurements (*14*). This work also showed that the peptide self-associated in the membrane at interfacial regions around cholesterol-rich domains. We suggest that a similar situation results in the stabilization of the cholesterol-rich domains found in the present study.

The results reported in this study demonstrate that cholesterol markedly alters the interaction of *N*-acetyl-LWYIK-amide with a bilayer. This is most directly indicated by the NMR results that generally show larger NOE cross-peaks between the aromatic protons and the protons from the lipid (Figures 8 and 9). In contrast, the quaternary ammonium group in the lipid headgroup has a greater interaction with the aromatic groups of the peptide in the bilayer without cholesterol (Figure 10). Thus, the peptide is less inserted into the bilayer in the absence of cholesterol. However, even in the presence of cholesterol, evidence from the intrinsic fluorescence emission of the Trp residue of the peptide indicates that the peptide is located near the membrane−water interface. The NOE observed with the terminal methyl group likely results from molecular motion of the peptide and lipid that allows for occasional access of the aromatic groups to the center of the bilayer. This transient insertion of the peptide allowing interaction with the terminal methyl group of the acyl chain occurs more frequently when cholesterol is present. This is opposite to what would be expected a priori since cholesterol is known to order liquid crystalline membranes and prevent penetration of substances into the bilayer. However, it has been found that phospholipids experience a higher axial mobility in the presence of cholesterol than in pure lipid bilayers (*47*). It has been suggested that cholesterol reduces chain entanglement near the center of the bilayer, allowing the terminal methyl end of the acyl chain greater access to regions closer to the membrane interface. Hence, it is likely that rather than the peptide occasionally penetrating to the center of the bilayer, cholesterol increases the spacing between phospholipids, allowing the acyl chains to reverse direction.

The precise molecular basis for the preferential interaction of *N*-acetyl-LWYIK-amide with cholesterol is likely a consequence of the presence of amino acids with aromatic side chains. These aromatic rings would provide flat, planar structures that could stack with a portion of the ring system of cholesterol. The location of the aromatic groups is largely near the membrane interface, as is generally found with other peptides and proteins (*48*). In addition, the ^{13}C resonances most affected by the peptide correspond to atoms of the lipid that are located near the membrane interface (Table 4). Finally, the fluorescence emission maximum from the Trp

of the peptide, when it is in a membrane, is not very different from that of a solution in methanol, indicating that it is in an environment with a polarity expected near the membrane interface. This is consistent with *N*-acetyl-LWYIK-amide interacting with the A ring of cholesterol and is likely to be the basis of the mechanism by which this peptide sequesters cholesterol into domains. The existence of this interaction is not sufficient to cause this peptide to bind specifically only to membranes containing cholesterol. However, in the region of the membrane in which the local concentrations of peptide and cholesterol are high, this interaction is sufficiently strong to cause the segregation of cholesterol into domains. It has been noted that basic amino acid residues will interact with aromatic amino acid side chains that are on the same side of a helix (*49*). Both LWYIK and KYWFYR have clusters of aromatic residues and basic amino acid residues, yet the former peptide has some preferential interaction with cholesterol but the latter does not. This must depend on the conformation of the peptide and the manner in which it inserts into the membrane. The Trp emission spectra of both peptides are comparable (Figure 14), although the intensity of *N*-acetyl-LWYIK-amide is more sensitive to lipid. The NMR spectra clearly indicate that one of the Tyr residues of KYWFYR is less inserted into the membrane than any residue of LWYIK. Thus, despite some similarities in the structure of these two peptides, it is not surprising that they differ in the degree of their interaction with cholesterol-rich domains.

ACKNOWLEDGMENT

We are very grateful to Steven O. Smith of SUNY Stony Brook for his advice and suggestions regarding the application of the NMR methodologies to this study. We are grateful to Dr. José Nieva for providing us with his manuscript prior to publication.

REFERENCES

1. Epand, R. M. (2003) *Biochim. Biophys. Acta 1610*, 155−156.
2. Brown, D. A., and London, E. (1998) *Annu. Rev. Cell Dev. Biol. 14*, 111−136.
3. McIntosh, T. J., Vidal, A., and Simon, S. A. (2003) *Biophys. J. 85*, 1656−1666.
4. Mahfoud, R., Garmy, N., Maresca, M., Yahi, N., Puigserver, A., and Fantini, J. (2002) *J. Biol. Chem. 277*, 11292−11296.
5. Fantini, J. (2003) *Cell Mol. Life Sci. 60*, 1027−1032.
6. Mahfoud, R., Mylvaganam, M., Lingwood, C. A., and Fantini, J. (2002) *J. Lipid Res. 43*, 1670−1679.
7. Epand, R. M., Maekawa, S., Yip, C. M., and Epand, R. F. (2001) *Biochemistry 40*, 10514−10521.
8. Maekawa, S., Sato, C., Kitajima, K., Funatsu, N., Kumanogoh, H., and Sokawa, Y. (1999) *J. Biol. Chem. 274*, 21369−21374.
9. Ramachandran, R., Heuck, A. P., Tweten, R. K., and Johnson, A. E. (2002) *Nat. Struct. Biol. 9*, 823−827.
10. Shimada, Y., Maruya, M., Iwashita, S., and Ohno-Iwashita, Y. (2002) *Eur. J. Biochem. 269*, 6195−6203.
11. Waheed, A. A., Shimada, Y., Heijnen, H. F., Nakamura, M., Inomata, M., Hayashi, M., Iwashita, S., Slot, J. W., and Ohno-Iwashita, Y. (2001) *Proc. Natl. Acad. Sci. U.S.A. 98*, 4926−4931.
12. Li, H., and Papadopoulos, V. (1998) *Endocrinology 139*, 4991−4997.
13. Salzwedel, K., West, J. T., and Hunter, E. (1999) *J. Virol. 73*, 2469−2480.
14. Saez-Cirion, A., Nir, S., Lorizate, M., Agirre, A., Cruz, A., Perez-Gil, J., and Nieva, J. L. (2002) *J. Biol. Chem. 277*, 21776−21785.
15. Liao, Z., Cimakasky, L. M., Hampton, R., Nguyen, D. H., and Hildreth, J. E. (2001) *AIDS Res. Hum. Retroviruses 17*, 1009−1019.
16. Sarin, P. S., Gallo, R. C., Scheer, D. I., Crews, F., and Lippa, A. S. (1985) *N. Engl. J. Med. 313*, 1289−1290.
17. Schaffner, C. P., Plescia, O. J., Pontani, D., Sun, D., Thornton, A., Pandey, R. C., and Sarin, P. S. (1986) *Biochem. Pharmacol. 35*, 4110−4113.
18. Vincent, N., Genin, C., and Malvoisin, E. (2002) *Biochim. Biophys. Acta 1567*, 157−164.
19. Woodman, S. E., Schlegel, A., Cohen, A. W., and Lisanti, M. P. (2002) *Biochemistry 41*, 3790−3795.
20. Privalov, G., Kavina, V., Freire, E., and Privalov, P. L. (1995) *Anal. Biochem. 232*, 79−85.
21. Ames, B. N. (1966) *Methods Enzymol. 8*, 115−118.
22. Sober, H. A., Ed. (1970) In *Handbook of Biochemistry: Selected Data for Molecular Biology*, pp B-75−B-76, The Chemical Rubber Co., Cleveland, OH.
23. Forbes, J., Bowers, J., Shan, X., Moran, L., Oldfield, E., and Moscarello, M. A. (1988) *J. Chem. Soc., Faraday Trans. 84*, 3821−3849.
24. Guo, W., and Hamilton, J. A. (1996) *Biophys. J. 71*, 2857−2868.
25. Arnold, M. R., Kremer, W., Ludemann, H. D., and Kalbitzer, H. R. (2002) *Biophys. Chem. 96*, 129−140.
26. Bach, D., and Wachtel, E. (2003) *Biochim. Biophys. Acta 1610*, 187−197.
27. Epand, R. M., Hughes, D. W., Sayer, B. G., Borochov, N., Bach, D., and Wachtel, E. (2003) *Biochim. Biophys. Acta 1616*, 196−208.
28. Brzustowicz, M. R., Cherezov, V., Zerouga, M., Caffrey, M., Stillwell, W., and Wassall, S. R. (2002) *Biochemistry 41*, 12509−12519.
29. Brzustowicz, M. R., Stillwell, W., and Wassall, S. R. (1999) *FEBS Lett. 451*, 197−202.
30. Epand, R. M., Epand, R. F., Bain, A. D., Sayer, B. G., and Hughes, D. W. (2003) *Magn. Reson. Chem.* (in press).
31. Loomis, C. R., Shipley, G. G., and Small, D. M. (1979) *J. Lipid Res. 20*, 525−535.
32. Epand, R. M., Bach, D., Epand, R. F., Borochov, N., and Wachtel, E. (2001) *Biophys. J. 81*, 1511−1520.
33. Epand, R. M. (2003) *Biophys. J. 84*, 3102−3110.
34. Epand, R. M., Bach, D., Borochov, N., and Wachtel, E. (2000) *Biophys. J. 78*, 866−873.
35. Loomis, C. R., Shipley, G. G., and Small, D. M. (1979) *J. Lipid Res. 20*, 525−535.
36. Zhang, W., Crocker, E., McLaughlin, S., and Smith, S. O. (2003) *J. Biol. Chem. 278*, 21459−21466.
37. Epand, R. M., Bain, A. D., Sayer, B. G., Bach, D., and Wachtel, E. (2002) *Biophys. J. 83*, 2053−2063.
38. White, S. H., Ladokhin, A. S., Jayasinghe, S., and Hristova, K. (2001) *J. Biol. Chem. 276*, 32395−32398.
39. De Planque, M. R. R., Bonev, B. B., Demmers, J. A. A., Greathouse, D. V., Koeppe, R. E., II, Separovic, F., Watts, A., and Killian, J. A. (2003) *Biochemistry 42*, 5341−5348.
40. Yau, W. M., Wimley, W. C., Gawrisch, K., and White, S. H. (1998) *Biochemistry 37*, 14713−14718.
41. Epand, R. M., Maekawa, S., Yip, C. M., and Epand, R. F. (2001) *Biochemistry 40*, 10514−10521.
42. Epand, R. M., Braswell, E. H., Yip, C. M., Epand, R. F., and Maekawa, S. (2003) *Biochim. Biophys. Acta 1650*, 50−58.
43. Epand, R. M., Maekawa, S., Yip, C. M., and Epand, R. F. (2001) *Biochemistry 40*, 10514−10521.
44. Dietrich, C., Bagatolli, L. A., Volovyk, Z. N., Thompson, N. L., Levi, M., Jacobson, K., and Gratton, E. (2001) *Biophys. J. 80*, 1417−1428.
45. Veatch, S. L., and Keller, S. L. (2003) *Biophys. J. 84*, 725−726.
46. Epand, R. M., Maekawa, S., Yip, C. M., and Epand, R. F. (2001) *Biochemistry 40*, 10514−10521.
47. Trouard, T. P., Nevzorov, A. A., Alam, T. M., Job, C., Zajicek, J., and Brown, M. F. (1999) *J. Chem. Phys. 110*, 8802−8818.
48. White, S. H., and Wimley, W. C. (1998) *Biochim. Biophys. Acta 1376*, 339−352.
49. Andrew, C. D., Bhattacharjee, S., Kokkoni, N., Hirst, J. D., Jones, G. R., and Doig, A. J. (2002) *J. Am. Chem. Soc. 124*, 12706−12714.
50. Saez-Cirion, A., Arrondo, J. L. R., Gomara, M. J., Lorizate, M., Iloro, I., Melikyan, G., and Nieva, J. L. (2003) *Biophys. J.* (in press).
51. Liao, Z., Graham, D. R., and Hildreth, J. E. (2003) *AIDS Res. Hum. Retroviruses 19*, 675−687.

BI035587J